Food Chemistry 360 (2021) 130049

Contents lists available at ScienceDirect

Food Chemistry

journal homepage: www.elsevier.com/locate/foodchem

Characterization of Tempranillo negro (VN21), a high phenolic content grapevine Tempranillo clone, through UHPLC-QqQ-MS/MS polyphenol profiling

Carolina Royo [1], Yolanda Ferradás [1], José Miguel Martínez-Zapater, Maria-Jose Motilva [*]

Instituto de Ciencias de la Vid y del Vino-ICVV (Consejo Superior de Investigaciones Científicas-CSIC, Universidad de La Rioja, Gobierno de La Rioja), Finca La Grajera, Ctra. de Burgos Km. 6 (LO-20, - salida 13), 26007 Logroño (La Rioja), Spain

ARTICLE INFO

Keywords:
Anthocyanins
Berry phenolic composition
Wine phenolic composition
Somatic variation
Phenolic compounds
Stilbenes
Tempranillo
Vitis vinifera

ABSTRACT

Grapevine cultivar and clone genotype is an important factor in the phenolic composition of wine. In this study, a new intense dark black berry color variant of Tempranillo, known as Tempranillo negro or VN21, is described. A targeted chromatographic approach based on UHPLC-QqQ-MS/MS was used to study the anthocyanins and non-colored phenols of the grape berry (skin and seeds) and wine. RJ43, one of the most cultivated clones in D.O.Ca. Rioja (Spain), was analyzed for comparison. Results suggest that the unique color of the grape skin in Tempranillo negro could be explained by higher concentrations of peonidin and cyanidin derivatives. This genotype accumulated anthocyanins in the seeds. Those differences in the berry were enhanced in the VN21 wines, which displayed notably higher concentrations of anthocyanins, and significantly increased contents of proanthocyanidins and stilbenes. This study exemplifies the application of phenol chromatographic analyses of spontaneous somatic variants to grapevine clonal selection.

1. Introduction

Phenolic compounds are intrinsic components of grape berries and derived products, particularly wine, and contribute to their organoleptic properties. Phenolic compounds constitute a heterogeneous family of chemical compounds with multiple components (Garrido & Borges, 2013) that can be separated into two broad categories, flavonoids and non-flavonoids (Harbone, Mabry & Mabry, 1975). Flavonoids play an important role on the sensorial attributes of wine, being responsible for color, bitterness, astringency and flavor (Cuadros-Inostroza, Verdugo-Alegría, Willmitzer, Moreno-Simunovic, & Vallarino, 2020). The flavonoid group includes strongly pigmented anthocyanins, as well as colorless flavanols (procyanidins) and flavonols (Garrido & Borges, 2013). On the other hand, the non-flavonoids include the hydroxybenzoic and hidroxycinnamic acids and stilbenoids such as resveratrol. Non-flavonoids enhance and stabilize the color of red wines, and contribute to its flavour (Cuadros-Inostroza et al., 2020). Some of them (e.g. resveratrol) exhibit potent biological activity (Restani et al., 2021).

The phenolic profile of wines can be used as a fingerprint for their differentiation or complexity, according to the geographical origin, vintage, vine variety and even clonal diversity (Fraige, Pereira-Filho, & Carrilho, 2014; Lukić, Radeka, Budić-Leto, Bubola, & Vrhovsek, 2019; Pantelić et al., 2016). The qualitative and quantitative phenolic composition of grapes and wines depends on multiple factors, such as cultivar, growing conditions (climate or soil) and degree of berry ripeness (He et al., 2010; Mattivi, Guzzon, Vrhovsek, Stefanini, & Velasco, 2006; Pinasseau et al., 2017). In addition, most of the studies in the literature over recent years have shown that the genotype effect of cultivar and clone is an important factor in the phenolic composition of wines (Muñoz et al., 2014; Pantelić et al., 2016; Samoticha, Jara-Palacios, Hernández-Hierro, Heredia, & Wojdylo, 2018). Therefore, clonal selection based on intra-cultivar genetic diversity has drawn considerable attention for helping to obtain red wines with high phenolic contents, these being responsible for key quality aspects of the wine, such as organoleptic properties, stability, complexity and health benefits.

Berry color has been a valuable trait throughout grapevine domestication, breeding and selection (Fang, Jogaiah, Guan, Sun, & Abdelrahman, 2018). Intracultivar variation for the presence or absence of color related to the anthocyanin content has been widely described in

* Corresponding author.
E-mail address: motilva@icvv.es (M.-J. Motilva).
[1] These authors contributed equally to the article.

https://doi.org/10.1016/j.foodchem.2021.130049
Received 10 February 2021; Received in revised form 4 May 2021; Accepted 4 May 2021
Available online 11 May 2021

many cultivars (Azuma, 2018). The anthocyanin profile is also variable both qualitatively and quantitatively between different black berry cultivars. In fact, anthocyanin and phenolic skin contents can respectively vary by up to 2.7 or 5.2-fold (Biniari et al., 2020; Eshghi, Salehi, & Karami, 2014; Pomar, Novo, & Masa, 2005). Diversity in phenolic profiles has also been identified in different clones of the same grapevine cultivar. Specifically, differences among clones from different cultivars results in variations in the total anthocyanin content to the same order as those observed between cultivars, up to 2.4-fold among six Barbera clones (Ferrandino & Guidoni, 2010) and 131 Malbec clones (Muñoz et al., 2014), or 1.8-fold among ten Pinot Noir clones (Castagnoli & Vasconcelos, 2006). The maximum differences in the total phenolic content rose to 2.7-fold within four Merlot clones, or up to three-fold among four clones of Cabernet Franc (Pantelić et al., 2016).

Those differences in the anthocyanin and phenolic contents in the grape skin can be identified in wines, either intensified or reduced during the winemaking process. The total anthocyanins in twenty Greek red wines ranged from 18.6 to 1011.8 mg/L, and the total phenolic compounds from 77 to 475 mg/L (Kallithraka, Tsoutsouras, Tzourou, & Lanaridis, 2006). The phenolic composition of wines from ten Cabernet Franc clones showed a range of anthocyanin contents from 475 to 601 mg/L, and total phenols (D280) from 45.7 to 58 mg/L (Van Leeuwen, Roby, Alonso-Villaverde, & Gindro, 2013). A comparison of the monomeric flavan-3-ols contents of three monovarietal wines varied from 32.8 mg/L in Tempranillo Tinto up to 51.1 mg/L in Graciano, and the respective levels of catechin being 22, 21 and 33% in Tempranillo, Graciano, and Cabernet Sauvignon (Monagas, Gómez-Cordovés, Bartolomé, Laureano, & da Silva, 2003).

Tempranillo is the main red wine grape variety grown in Spain, and different clonal selections of this cultivar have been obtained since 1976. Regarding the variation in berry color, a bud sport mutation producing white berries was detected in 1988. This was the base for generating a new Tempranillo Blanco white wine cultivar (Martínez, Vicente, Martínez, Chavarri & García-Escudero, 2006). This mutation resulted from several chromosomic rearrangements and a loss of genetic material (Carbonell-Bejerano et al., 2017). Genetic variation for other traits that improve quality features related to adaptation to climate change or oenological properties have also been described (Arrizabalaga et al., 2018; Mendes Lemos, Machado, Egea-Cortines, & Barros, 2020). Clonal variation of the anthocyanin composition in Tempranillo has hardly been analyzed. Only one study reported slightly significant differences in the skin content of delphinidin-glucoside, peonidin-glucoside, malvidin-acetylglucoside, and malvidin-*p*-coumarylglucoside between six clones (Revilla, García-Beneytez, & Cabello, 2009). Those differences ranged in ratio between 1.1 and 1.4-fold in each compound from the same vintage. Moreover, the differences observed among clones were not expressed in their wine composition.

To the best of our knowledge, no detailed qualitative and quantitative analysis of individual phenolic compounds has been carried out on Tempranillo clones. In the present study, a new variant of Tempranillo, known as Tempranillo negro (black) or VN21, that displays an intense dark black berry color is described. To characterize this phenotype, a targeted chromatographic approach based on ultra-high performance liquid chromatography with tandem mass spectrometry (UHPLC-QqQ-MS/MS) was used to study the anthocyanin and non-colored phenol profiles of the grape berry (skin and seeds). A reference Tempranillo clone, RJ43, one of the most widely grown clones in D.O.Ca. Rioja (Spain), was also analyzed for comparison. In addition, how the winemaking process affects the profile of the anthocyanin and non-colored phenols in VN21 wines was determined. The results point out important differences in the phenolic profile of the VN21 clone, which generate new wine features in terms of color and phenol composition.

2. Material and methods

2.1. Chemicals and reagents

Cyanidin-3-*O*-glucoside, malvidin-3-*O*-glucoside, resveratrol, (−)-epicatechin, dimer B2 and quercetin were purchased from Extrasynthese (Genay, Cedex, France). (+)-Catechin, *p*-hydroxybenzoic acid, *p*-hydroxyphenylacetic acid, 3,4-dihydroxybenzoic acid (protocatechuic acid), *p*-coumaric acid, gallic acid, caffeic acid, ferulic acid, vanillic acid and syringic acid were from Sigma-Aldrich (St. Louis, MO, USA). Methanol (HPLC grade), formic acid (HPLC grade) and acetonitrile (HPLC grade) were purchased from VWR Chemicals BDH Prolabo (Leuven, Belgium) and glacial acetic acid (HPLC grade) was purchased from Scharlab Chemie (Sentmenat, Catalonia, Spain). The water was Milli-Q quality (Millipore Corp, Bedford, MA, USA). Stock solutions of standard compounds were prepared by dissolving each compound in methanol at a concentration of 1000 mg/L, and stored in a dark flask at −20 °C. For the preparation of calibration curves, three cocktail standards were readied: anthocyanins (cyanidin-3-*O*-glucoside, malvidin-3-*O*-glucoside), flavonoids ((−)-epicatechin, dimer B2 and quercetin), and resveratrol and phenolic acids (*p*-hydroxybenzoic acid, *p*-hydroxyphenylacetic acid, 3,4-dihydroxybenzoic acid (protocatechuic acid), *p*-coumaric acid, gallic acid, caffeic acid, ferulic acid, vanillic acid, syringic acid). The three calibration curves were prepared in the range from 0 to 10 ppm.

2.2. Plant material

Vitis vinifera L. cv. 'Tempranillo' clones, VN21 and RJ43, were trained in single cordon Royat system in an experimental vineyard belonging to Vitis Navarra® Genética y Plantas de Vid at Vergalijo (Navarra, Spain) (location coordinates VN21: 42.462012110147775, −1.8043137124582738; RJ43 location: 42.46465728706511, −1.804570898827128). The vineyard was supported by irrigation and controlled release of NPK 15-5-20 fertilizer. In this plot, the soil is loam according to the USDA soil texture triangle. The soil was characterized by high calcium low mineralization rate, low activity, low nutrients amount and high carbonate level. All the vines were 7-year-old plants managed under the same conditions in the same field. During development (from 8/08/2019 to 17/09/2019) berries were collected from different vines to measure the total soluble sugars (TSS, °Brix) (Atago 3415 WM-7 Digital Wine Refractometer, U.S.A, Inc.) to follow ripening. The grapes were picked on September 17th, 2019 coinciding with the harvest of the DOC La Rioja. Mature bunches were harvested from 20 plants (average 50 Kgs for each Tempranillo clone) and immediately moved to the experimental winery for the winemaking process. All bunches collected for each genotype (VN21 and RJ43) were combined and divided into three winemaking replicates. Before winemaking, two clusters per clone were randomly sampled for each winemaking replicate and stored at −80 °C for subsequent UHPLC-MS analysis. In addition, the day after picking, 30 berries were stored at 4 °C to analyses °Brix and other characteristics of the grapes (Supplementary Table 1S).

Berry diameter was measured using an Absolute Digital Caliper (Mitutoyo, Japan), and the skin surface area was calculated as round fruits. Berry skin color was measured with a portable tristimulus Chroma Meter model CR-400 (Konica Minolta, Osaka, Japan) with an 8-mm-diameter viewing area. For each clone, ten berries were randomly chosen for measuring the CIELab coordinates and every berry was measured four times in opposing positions. The results of the tristimulus values of the CIELab chromatic parameters were expressed according to those of the International Commission on Illumination. L* stands for lightness (0 = black, 100 = white), a* indicates the red (positive)/green (negative) coordinate, and *b** represents the yellow (positive)/blue (negative) coordinate.

For wine, color was measured with an Agilent Cary 60 UV–Vis spectrometer (Agilent, Richardson, TX, USA) equipped with the UV

Agilent Cary 60 computer software package, version 5.0.0.999. The color coordinates (CIELab) were calculated according to the CIE D65 illuminant for the wavelength range from 400 to 780 nm, using crystal cells. The total polyphenol index (IPT) was calculated for a wavelength of 280 nm, using quartz cells.

2.3. Small-lot winemaking procedure

Three small-lot wine replicates per Tempranillo clone (VN21 and RJ43) were made according to the small-scale winemaking procedure established in the experimental winery of the ICVV (Instituto de Ciencias de la Vid y del Vino-ICVV, La Rioja, Spain). The winemaking was conducted following the traditional alcoholic (AF) and malolactic (MLF) fermentations. Bunches were de-stemmed and crushed. Free 50 mg/L sulphur dioxide (SO_2) (added as an 8% solution of potassium metabisulfite) were added to the must, and then it was inoculated with commercial *Saccharomyces cerevisiae* yeast strains Uvaferm VRB® (Lallemand, St Simon, France) (20 g/hL) following the manufacturer's instructions. The wines were fermented in a temperature controlled room (~20 °C) for 9 days and the cap was plunged down every day. The fermentation temperature and density (g/L) were monitored daily and when the ferments reached a density value of approximately 990–1000 g/L the wines were pressed in a small water bag press (~1000 kPa) and transferred to glass flagons. The wines were kept in a room at 20 °C for approximately one week until the reducing sugars were below 2 g/L (Supplementary Table 2S). For the MLF under controlled conditions at 20 °C, the wines were inoculated with the commercial bacteria Oenococcus oeni strain LalvinSilka™ (Lallemand) (1 g/hL). MLF evolution was followed by analyzing the malic acid and glucose/fructose contents (Supplementary Table 2S). The parameters related to the fermentative process, such as the residual sugars (density), the fermentative effectiveness (sugar consumed related to the ethanol produced) and the fructophilic character (glucose/fructose) were assessed. The malic fermentation was monitored by the malic acid concentration. These parameters were measured enzymatically in a MIURA One enological analyzer (TDI Barcelona, Spain) following the supplier's instructions. The wines were stored at 4 °C for 18 days to stabilize, then potassium metabisulfite was added for a final SO_2 concentration of 50 mg/L and they were bottled (0.75 L).

Aliquots of musts or fermenting wines were collected during AF, at the end of MLF and immediately before bottling. A total of ten samples were collected during the process (Supplementary Table 2S). Immediately after the samples were collected, they were centrifuged for 10 min at 20 °C and 4000 rpm in a Sorvall LYNX 4000 Superspeed Centrifuge (Thermo Scientific™, Madison, WI, USA) and then stored at −80 °C until their chromatographic analysis.

2.4. Grape berry sample preparation for the determination of phenolic compounds

Just before UHPLC-MS, the grape samples (stored at −80 °C) were lyophilized and phenolic compounds extracted. Three biological replicates of 18 grape berries per clone were selected and washed. The separated skin and seeds were weighed on a precision balance and used for the extraction process. The skin and seeds were frozen, freeze-dried (Lyophilizer TELSTAR LyoQuest, Terrassa, Spain), and homogenized to a fine powder. The samples were packed individually into sealed plastic tubes and stored in vacuum until used. The phenolic compounds of the skin and seeds were extracted using solid–liquid extraction (SLE). Briefly, lyophilized grape skin (100 mg) and seed (100 mg) were weighed in a falcon tube (15 mL). Then, 10 mL of methanol/Milli-Q water/formic acid (79:20:1, v/v/v) were added as the extraction solvent. The samples were vortexed and macerated overnight at 4 °C in the dark. Later, the samples were sonicated (5 min at 20 °C, 40 Hz frequency) using an Ultrasons P. Selecta sonicator bath (J.P. Selecta S.A., Barcelona, Spain). The extracts were centrifuged at 9000 rpm for 10 min at 20 °C in a Sorvall LYNX 4000 Superspeed Centrifuge (Thermo Scientific™, Madison, WI, USA) to collect the supernatants. The extraction procedure was repeated twice, adding 5 mL of extraction buffer to the solid residue, sonicating and centrifuging. The supernatants of each cycle were gathered, adjusted to 20 mL with the extraction solvent and stored at −80 °C until their chromatographic analyses.

2.5. Ultra-performance liquid chromatography coupled to tandem mass spectrometry (UHPLC-QqQ-MS/MS)

The samples of grape berry skin and seed phenol extracts (Section 2.4), musts and fermenting wines (different phases of the winemaking process) (Supplementary Table 2S) were filtered with LLG Syringe Filters SPHEROS, PTFE, 0.22 μm pore size (LLG Labware, Meckenheim, Germany) and analyzed by ultra-high performance liquid chromatography with triple-quadrupole mass spectrometry (UHPLC/QqQ-MS/MS) based on the method described by Motilva et al. (2016) with modifications. The LC analyses were carried out on a Shimadzu Nexera liquid chromatograph (Shimadzu Corporation, Japan), coupled to an AB Sciex 3200QTRAP® mass spectrometer (Sciex, USA). Two chromatographic methods were used for the analysis of 1) anthocyanins, and 2) the rest of the non-colored phenolic compounds. In the two chromatographic methods, the flow rate was 0.45 mL/min, and 2.5 μL of all the phenolic extracts analyzed were injected. The autosampler and oven temperatures were respectively 5 °C and 40 °C.

For the analysis of the anthocyanins and non-colored phenolic compounds, the analytical column used was a Waters AcQuity BEH C_{18} (100 mm × 2.1 mm i.d., 1.7 μm,) equipped with a VanGuard™ Pre-Column Acquity BEH C_{18} (5 × 2.1 mm, 1.7 μm) from Waters (Milford, MA, USA). Mobile phase solvents were Milli-Q water, LCMS grade acetonitrile and LCMS grade formic acid. For the analysis of the anthocyanins, the mobile phase was 2% formic acid in water (eluent A), and 2% formic acid in acetonitrile (eluent B). The elution gradient was: 0–0.5 min, 1% B isocratic; 0.5–1.5 min, 1–8% B; 1.5–4 min, 8% B isocratic; 4–5 min, 8–12% B; 5–5.5 min, 12% B isocratic; 5.5–6 min, 12–14% B; 6–7 min, 14% B isocratic; 7–9 min, 14–22% B; 9–12 min, 22–30% B; 12–13.5 min, 30–90% B; 13.5–14.5 min, 90% B isocratic; 14.5–15 min, 90–1% B; 15–18 min, 1% B isocratic. For the analysis of the rest of the non-colored phenolic compounds, the mobile phase was 0.1% formic acid in water (eluent A), and 0.1% formic acid in acetonitrile (eluent B). The elution gradient was the same as for anthocyanins.

Tandem MS analyses were carried out on a 3200QTRAP triple quadrupole mass spectrometer (AB Sciex, USA) equipped with an electrospray ionization source (ESI Turbo V™ Source). Ionization was achieved using the electrospray (ESI) interface operating in the positive mode $[M-H]^+$ for the analysis of anthocyanins, and in the negative mode $[M-H]^-$ for the rest of the phenolic compounds. The data was acquired through multiple reaction monitoring (MRM). The ionization source parameters were an ion spray voltage of ±4.5 kV, the source temperature was 700 °C and the gas pressures were curtain gas 50 psi; GS1 50 psi and GS2 60 psi). Nitrogen (>99.99% purity, degasified liquid nitrogen from a tank, Air Liquide, USA) was used as the source and collision gases. Two MRM transitions were studied, the most sensitive one being selected for quantification and a second one for confirmation purposes. The retention time and MRM transitions for quantification and identification, including the individual Declustering potential (DP), Entrance potential (EP), Collision cell entrance potential (CEP), Collision energy (CE) and Collision cell exit potential (CXP), for each phenolic compound, are shown in Supplementary Table 3S. The dwell time established for each transition was optimized through the chromatogram with the Scheduled MRM tool by means of the retention time, MRM detection window of 60 s and a target scan time of 1 s. Data acquisition was carried out with the Analyst ® 1.6.2 software (AB Sciex, USA). Compounds were identified by comparing their chromatographic behavior and mass spectra with those of authentic standards and the literature data.

When no standards were available, the phenolic compounds from wine/grape extracts were identified by using the MS detector system. Then, in order to determine their MRMs, MS analyses of these samples were carried out. These were based on the full-scan mode in the MS mode, and the daughter scan mode in the MS/MS mode. First, the analyses were performed in the full-scan mode, from 80 to 800 *m/z*, by applying cone voltages ranging from 20 to 60 V. When low cone voltages were applied, the MS spectrum gave information about the precursor ion, the $[M-H]^-$ or the $[M+H]^+$. In contrast, when high cone voltages were applied, specific fragment ions were generated and the MS spectrum gave information about their structure. Then, in order to determine the specific fragments, the daughter scan mode in the MS mode was used with collision energies ranging from 5 to 30 eV. Then, the MRM used for quantification was the transition with the precursor ion and the fragment ion with most sensitivity with the optimum cone voltage, and the collision energy.

Some of the anthocyanins and non-colored phenolic compounds were quantified using the calibration curves of their corresponding pure commercial standards. The other compounds were tentatively quantified using the calibration curves of standards with similar chemical structures (Supplementary Table 3S). Statistic parameters of the calibration curves, and LODs and LOQs provided for each compound applied in the calibration curve(s) are shown in Supplementary Tables 4S and 5S, respectively.

Initially, all samples were injected without dilution. In those compounds for whom the intensity of the ESI-MS/MS spectrum was outside the linearity range of the calibration curve, the samples were diluted 10 times. The skin and seed extracts were diluted with a solution of methanol/Milli-Q water/formic acid (79:20:1, v/v/v), and the wines diluted with a solution of Milli-Q water/ethanol (85:15, v/v). The results were expressed as mg compound/Kg grape skin or seed, and mg/L must or wine, respectively.

2.6. Statistical analysis

The phenol concentration values were reported as means (n = 3). All data were analyzed with the SPSS software (version 26.0 for Windows; IBM). Statistical comparisons between Tempranillo clones (VN21 and RJ43) to determine the significance of differences were assessed with a two-sided Student's *t*-test for grape skin, grape seed and wines. Statistical comparisons to evaluate the evolution of the phenolic compounds during the winemaking process for each grapevine clone were assessed by one-way analysis of variance (ANOVA) followed by Tukey's b test, p-values < 0.05.

3. Results and discussion

3.1. Phenotypic characterization of Tempranillo negro (VN21)

3.1.1. Basic phenotypic features

In a recent selection of Tempranillo clones at Vitis Navarra SAT (Larraga, Navarra, Spain), one clone (VN21) (Supplementary Graphic 1S) displayed a deeper blue-black color than the reference Tempranillo clones exemplified here by RJ43 (one of the most widely cultivated clones in the D.O.Ca. Rioja) (Martínez-García, Vicente Renedo, & Martínez Martínez, 2000). In addition to the visual appearance observed in the field, the VN21 clone could also be distinguished by more intense brightness of the berry skin (Fig. 1A), a shorter ripening cycle and higher sugar content in every development stage according to the BBCH scale (Lorenz et al., 1995) (Fig. 1B). Moreover, despite similar berry weight and number of seeds per berry, VN21 produced abnormal red seeds with limited endosperm development and lignification and unable to germinate (Fig. 1C). Their total seed weight per berry was lower than that observed in the reference clone RJ43 ($P < 0.001$) (Supplementary Table 1S).

Attempts were made to confirm the black visual appearance of the berries through measurement of their CIELab chromatic parameters, which are related to the anthocyanin composition of the grape skin, and it was analyzed whether those differential phenotypic features of the berries could also contribute to improving the color and phenolic composition of derived wines. The blue-black color observed in the VN21 berries (Fig. 1A) was confirmed by CIELab analyses (Fig. 1D). The higher a* (positive red) and b* (negative blue) absolute values, and the lower L* value were in agreement with the blue-black appearance of the VN21 grape berries. In parallel, the wines elaborated with VN21 also showed higher color intensity than RJ43 wines as confirmed by the analysis of the CIELab colorimetric parameters of wines (Fig. 1D). The VN21 showed lower a*, b*, and L* values than the RJ43 wines. This suggests a higher anthocyanin content in the Tempranillo negro wines. As Fig. 1E shows, the ΔE*ab value for these wines was two times higher

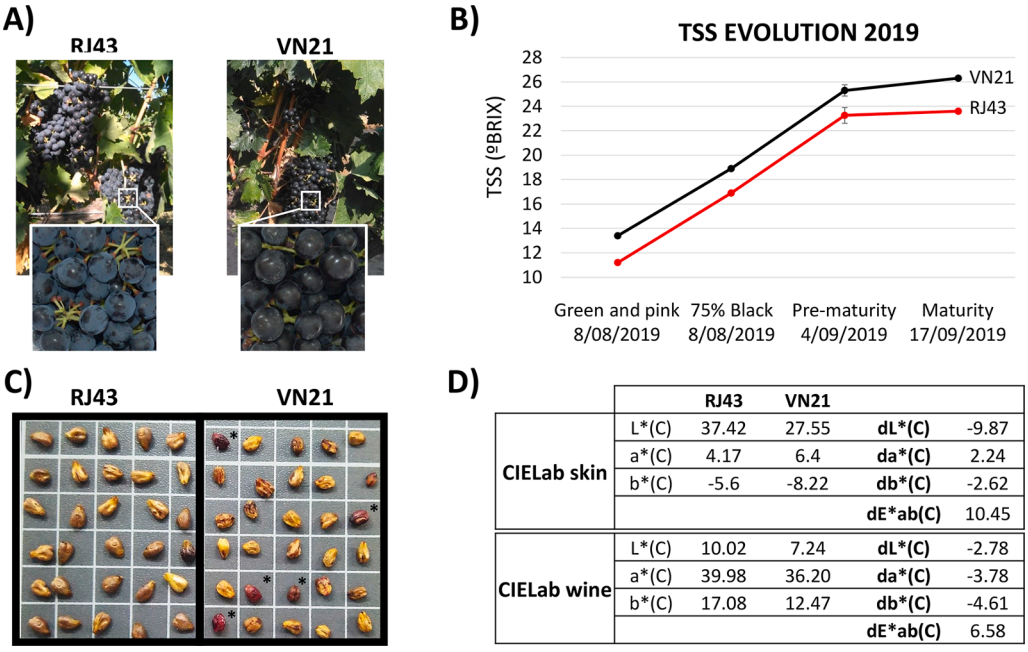

		RJ43	VN21		
CIELab skin	L*(C)	37.42	27.55	dL*(C)	-9.87
	a*(C)	4.17	6.4	da*(C)	2.24
	b*(C)	-5.6	-8.22	db*(C)	-2.62
				dE*ab(C)	10.45
CIELab wine	L*(C)	10.02	7.24	dL*(C)	-2.78
	a*(C)	39.98	36.20	da*(C)	-3.78
	b*(C)	17.08	12.47	db*(C)	-4.61
				dE*ab(C)	6.58

Fig. 1. Characterization of Tempranillo negro. A) Mature clusters of the reference RJ43 clone and the VN21 clone (Tempranillo negro), and zoomed berry detail. B) Sugar accumulation during ripening in RJ43 (red line) and VN21 (black line). The development stages were identified according to the BBCH scale Lorenz et al., 1995. C) Pictures of seeds extracted from RJ43 and VN21 mature berries* indicate the singular VN21 red seeds. D) RJ43 and VN21 CIELab results from the skin and wine, respectively. (For interpretation of the references to color in this figure legend, the reader is referred to the web version of this article.)

than the 2.7 CIELAB units which represent the red wine chromatic changes that can be perceived by the human eye (Martínez, Melgosa, Pérez, Hita, & Negueruela, 2001). Additionally, the total polyphenol index (IPT) was also higher in the VN21 (66.21) than in the RJ43 (48.80).

To explain the role of anthocyanins in the visual appearance of the VN21 berries and their CIELab colorimetric parameters, the anthocyanin composition and their quantitative pattern in VN21 grape skin and in the reference clone RJ43 were determined using targeted UHPLC-QqQ-MS/MS chromatography. In addition, to understand the differences in phenolic composition between the two Tempranillo clones better, the non-colored phenols belonging to the chemical classes of proanthocyanidins (flavan-3-ols), flavonols, phenolic acids (hydroxycinnamics and hydroxybenzoics) and stilbenes, were analyzed. Given the presence of the abnormal red seeds in the VN21 grapes (Fig. 1C), their anthocyanin and non-colored phenol content were also characterized.

3.1.2. *Anthocyanin composition of Tempranillo negro berry skins and seeds*

A wide range of anthocyanins have been identified in red grapes and wine, mainly derived from six anthocyanidins: cyanidin (orange red), peonidin (red), delphinidin (bluish red), pelargonidin (orange), petunidin and malvidin (bluish red) (He et al., 2010). The analysis of the berry skins showed similar qualitative composition of anthocyanins in the VN21 and RJ43, malvidin, delphidin and petunidin derivatives being the main anthocyanins quantified, mainly as monoglucosides (Table 1). Interestingly, the VN21 displayed statistically significant differences ($P < 0.01$) in the total content of peonidins and cyanidins (Table 1). Thus, differences in the proportions of peonidin (13.51% VN21 vs 8.92% RJ43) and cyanidin (4.13% VN21 vs 2.81% RJ43) derivatives, and to a lesser extent, of pelargonidin 3,6-diglucoside (Table 1), could explain differences in the visual appearance of the Tempranillo negro berries when compared with the Tempranillo clone RJ43. Similarly, a study by Revilla et al. (2009) in Tempranillo clones showed no significant differences in malvidin derivatives although there were in delphinidin-glucoside and peonidin-glucoside that were clone dependent. However, in this study, those differences were not visually conspicuous. In the opposite sense, Malbec clones with variations in the color intensity and total anthocyanin contents were found in their malvidin derivatives composition (Muñoz et al., 2014).

Anthocyanins do not accumulate in grapevine seeds and they were not detected in the seeds of the reference clone RJ43 (Table 1). However, the Tempranillo negro seeds showed significant anthocyanin accumulation, up to four times that detected in the seeds of the teinturier cultivar, Alicante Bouschet (Flaginella, Di Gaspero, & Castellarin, 2012). The red color often observed in the VN21 seeds (Fig. 1C) correlated with the presence of the monoglucoside derivatives of malvidin, peonidin, and cyanidin, although in much lower concentrations than those observed in the berry skin (Table 1).

3.1.3. *Non-colored phenol content of Tempranillo negro berry skins and seeds*

A wide range of non-colored phenols were identified and quantified in the berry skin and seeds. These belonged to the chemical classes of proanthocyanidins (flavanols), flavonols, phenolic acids (hydroxycinnamic and hydroxybenzoic acids) and stilbenes (Table 1 and Supplementary Table 6S). Tempranillo negro (VN21) showed significantly different concentrations for many of these compounds, particularly in the seeds, when compared with the RJ43 reference clone. The VN21 berry skin showed significantly lower proanthocyanidin content than the RJ43, specifically due to a significant reduction in the catechin, gallocatechin, and procyanidin dimer B1 contents (Table 1 and Supplementary Table 6S). Similarly, differences in skin flavanol content have been observed among clones from Cabernet Sauvignon, Marzemino, Merlot, Pinot Noir, Syrah and Teroldego cultivars (Mattivi, Vrhovsek, Masuero, & Trainotti, 2009), and in the flavanol composition in both the seed and skin among clones of the Rufete cultivar (García-

Table 1
Concentration of anthocyanins and non-colored phenols (proanthocyanidins, flavonols, hydroxycinnamic acids, hydroxybenzoic acids, and stilbenes) in grape skin and seeds of VN21 Tempranillo clone and reference RJ43.

Compound[1] (mg/Kg fresh weight)	Skin			Seed		
	RJ43	VN21	sig	RJ43	VN21	sig
Malvidin 3-glucs	3215.4	3049.6	ns	n.d.	20.74	***
M−3-(6″-acetyl)-glu	803.4	652.1	ns	n.d.	4.386	**
M−3-(6″-coum)-glu	665.4	406.5	**	n.d.	0.583	*
M−3-(6″-caffe)-glu	6.457	4.696	ns	n.d.	n.d.	
M−3−arabinoside	11.66	8.634	**	n.d.	n.d.	
Total malvidins	**4702**	**4121**	**ns**	**n.d.**	**25.71**	***
Petunidin-3-glu	1112.9	1234.4	ns	n.d.	0.339	**
Pet-3-(6″-acetyl)-glu	79.51	84.84	ns	n.d.	n.d.	
Pet-3-(6″-coum)-glu	204.9	142.3	**	n.d.	n.d.	
Pet-3- arabinoside	1.497	1.596	ns	n.d.	n.d.	
Total petunidins	**1399**	**1463**	**ns**	**n.d.**	**0.339**	**
Delphinidin-3-glu	1117	1278	ns	n.d.	0.070	ns
Del-3-(6″-acetyl)-glu	52.65	63.20	ns	n.d.	n.d.	
Del-3-(6″-coum)-glu	243.2	182.3	*	n.d.	n.d.	
Del-3,5-diglu	6.061	11.92	*	n.d.	n.d.	
Del-3- arabinoside	2.669	3.672	ns	n.d.	n.d.	
Total delphinidins	**1421**	**1539**	**ns**	**n.d.**	**0.070**	**ns**
Peonidin-3-glu	567.9	907.3	**	n.d.	58.66	**
Peo-3-(6″-acetyl)-glu	53.65	76.60	*	n.d.	5.390	**
Peo-3-(6″-coum)-glu	138.2	185.3	*	n.d.	11.69	**
Total peonidins	**759.7**	**1169.2**	**	**n.d.**	**75.74**	***
Cyanidin-3-glu	140.5	234.3	**	n.d.	10.66	**
Cy-3-(6″-acetyl)-glu	10.1	16.10	**	n.d.	0.680	*
Cy-3-(6″-coum)-glu	87.89	105.7	ns	n.d.	6.931	**
Cy-3-arabinoside	0.742	1.117	ns	n.d.	n.d.	
Total cyanidins	**239.2**	**357.2**	**	**n.d.**	**18.27**	**
Pelarg-3,6-diglu	0.260	2.006	***	n.d.	n.d.	
Total anthocyanins	**8522**	**8652**	**ns**	**n.d.**	**120.1**	***
Non-colored phenols						
catechin	54.10	43.21	*	557.5	4223.2	***
epicatechin	17.88	15.35	ns	490.4	3852.8	***
epicatechin-gallate	3.910	3.332	ns	137.2	590.4	**
gallocatechin	30.90	25.60	***	1.421	2.535	ns
epigallocatechin	14.78	15.62	ns	0.323	2.526	***
epigallocatechin-gallate	0.015	0.055	ns	0.094	0.066	ns
Total dimers (B1,B2, B3)	55.70	42.20	*	632.4	1998.4	**
Trimer	3.415	3.457	ns	13.28	34.88	*
Total proanthocyanidins	**180.7**	**148.9**	*	**1833.6**	**10704.8**	**
Total quercetins	2813.8	3487.1	*	37.34	171.3	**
Total kaempferols	639.0	904.9	ns	1.169	3.304	*
Total isorhamnetins	554.2	602.4	*	7.842	39.08	**
Total myricetins	455.2	409.2	*	0.456	4.413	**
sum minor flavonols	218.2	273.0	*	1.217	3.676	*
Total flavonols	**4680.3**	**5676.4**	**ns**	**48.03**	**221.8**	***
CA-hexose	3.139	4.351	ns	0.600	6.126	***
CU-hexose	10.85	10.60	ns	1.111	1.924	*
coutaric acid	115.4	91.19	*	2.129	5.969	**
caftaric acid	36.31	25.15	*	n.d.	n.d.	
fertaric acid	5.384	5.956	ns	0.702	0.934	ns
sum minor HC acids	0.129	0.276	ns	1.006	0.403	ns
Total HC acids	**171.2**	**137.5**	*	**5.547**	**15.38**	***
gallic acid	1.102	1.249	ns	92.84	361.1	***
GA-glucoside	15.91	18.69	ns	382.5	1542.5	***
PTC acid	118.8	127.2	ns	351.5	474.9	*
vanillic acid	4.860	4.641	ns	21.45	41.91	**
sum minor HB acids	3.658	3.481	ns	0.891	2.824	*
Total HB acids	**143.2**	**154.0**	**ns**	**849.1**	**2423.2**	***
resveratrol (*trans/cis*)	55.11	41.09	ns	2.706	24.81	***
piceid (*trans/cis*)	71.41	76.41	ns	4.646	18.67	***
piceatannol (*trans/cis*)	71.24	78.51	ns	0.839	3.866	**
astringin (*trans/cis*)	14.17	15.51	ns	6.469	9.563	ns
ε-viniferin	9.591	8.270	ns	0.258	0.665	*
ω-viniferin	71.06	76.91	ns	0.374	2.256	*
Total Stilbenes	**292.6**	**296.7**	**ns**	**15.29**	**59.83**	***

M: malvidin; Pet: petunidin; Del: delphinidin; Peo: peonidin; Cy: cyanidin; Pelarg: pelargonidin; -glu: glucoside; -coum: coumaroyl; caffe: caffeoyl; PA: proanthocyanidins; HC acids: hydroxycinnamic acids; CA: caffeic acid; CU:

coumaric acid; HB acids: hydroxybenzoic acids; GA: gallic acid; PCT: protocatechuic acid.

Asterisks denote significant differences between clones at the same stage according to Student's *t*-test (P < 0.05, n = 3): *, **and *** indicate significance at $p < 0.05$, $p < 0.01$ and $p < 0.001$, respectively; ns indicates no significant difference, n.d. indicates not detected values.

[1] Standard deviations were lower than 10% (n = 3)

Estévez, Alcalde-Eon, & Escribano-Bailón, 2017). Nevertheless, differences in the skin flavanol concentration between the VN21 and RJ43 clones observed in the present study were higher than those reported between the Merlot and Syrah varieties (Benbouguerra, Richard, Saucier, & Garcia, 2020).

When considering seeds, the significantly higher proanthocyanidin concentration ($P < 0.01$) detected in VN21 (Table 1) is notable at around six times higher than in the seeds of the RJ43. Catechin, epicatechin and dimer B2 were by far the most abundant constituents of the seed proanthocyanidins (Table 1 and Supplementary Table 6S). The high proanthocyanidin concentrations detected in Tempranillo negro seeds are at the levels described in some grape varieties like Merlot and Syrah (Benbouguerra et al., 2020; Rodríguez Montealegre, Romero Peces, Chacón Vozmediano, Martínez Gascueña, & García Romero, 2006) or in some clones from such other grape varieties as Cabernet Sauvignon, Merlot, Pinot Noir and Syrah (Mattivi et al., 2009). In this latter study, the variation in the proanthocyanidin contents of clones of the same variety was in the order of two-fold higher, while this increase was about six-fold in the VN21 seeds when compared with the RJ43. Previous studies have indicated that the flavanol or tannin accumulation in grapes depends on environmental factors (Pinasseau et al., 2017). In the present study, both Tempranillo clones were grown in the same plot under identical environmental conditions. This rules out a possible effect of environmental factors and indicates the specific activation of proanthocyanidin biosynthesis pathways in the VN21 grape seeds (Fig. 1C). Nevertheless, the higher proanthocyanidin content in the Tempranillo negro seeds could be related to its abnormal seed development.

Unlike proanthocyanidins, the most abundant in seeds, flavonols are the most abundant group of non-colored phenols in grape skin. The main flavonols quantified in the berry skin were quercetin, kaempferol, isorhamnetin and myricetin glycosylated mainly with glucose, but these were also linked with galactose, rutinose and glucuronic acid (Table 1 and Supplementary Table 6S). Despite no statistically significant differences in the total flavonol concentration in the skin, some of the individual flavonols (quercetin, isorhamnetin, and syringetin) were significantly higher in the VN21 berry skin (Supplementary Table 6S). In this sense, a study with the Barbera variety showed that the seasonal effect was marked on total flavonol content while the clones only showed an effect on some individual flavonols, such as myricetin-3-*O*-glucoside, quercetin-3-*O*-glucoside, and kaempferol-3-*O*-glucoside (Ferrandino & Guidoni, 2010). Regarding the seeds, the VN21 also showed a significantly higher total flavonol concentration (four-fold) ($P < 0.001$) than the RJ43, quercetin derivatives being the main flavonols in the seeds from both Tempranillo clones (Table 1).

Concerning the phenolic acids (hydroxycinnamic and hydroxybenzoic acids), the Tempranillo negro berry skin showed a lower concentration ($P < 0.05$) of total hydroxycinnamic acids than the RJ43. This was related to reduced contents of coutaric (coumaroyltartaric acid) and caftaric (caffeoyltartaric acid) acids (Table 1 and Supplementary Table 6S). However, in the seeds, which usually contain minor amounts of hydroxycinnamic acids, the VN21 showed a significant concentration three-fold higher than the RJ43 (Table 1 and Supplementary Table 6S).

Several types of hydroxybenzoic acids were detected in both the grape skin and seeds (Table 1 and Supplementary Table 6S). In the skin, the most abundant of these acids were protocatechuic acid and gallic acid-glucoside, and no significant differences were observed between the two Tempranillo clones (VN21 and RJ43). The content of hydroxybenzoic acids was higher in the seeds than in the skin, with the total level being significantly higher (three-fold) in the Tempranillo negro than in the RJ43. This was related to a higher content of gallic acid-glucoside and free gallic acid ($P < 0.01$) in the VN21 seeds (Table 1 and Supplementary Table 6S). Gallic acid has been described as a precursor of all hydrolyzable tannins and is among the condensed tannins (Garrido & Borges, 2013). Then, the higher contents of gallic acid derivatives in the VN21 seeds compared with the RJ43 could be related to the higher concentrations of procyanidins (dimers and trimer) detected (Table 1). Clonal variation has also been observed for the hydroxycinnamic acid content among clones of the Barbera cultivar (Ferrandino & Guidoni, 2010).

The last subclass of phenolic compounds analyzed was stilbenes. Different resveratrol derivatives were detected in the grape skin and seeds (Table 1 and Supplementary Table 6S) their concentration higher being in the skin than in the seeds of either of the Tempranillo clones studied. Most compounds accumulated to higher significant levels in the seeds of the VN21 than in the reference the RJ43 (Table 1 and Supplementary Table 6S).

To sum up, the analyses of anthocyanin and non-colored phenol composition in the Tempranillo negro berry skin showed no important differences with compared to the reference clone RJ43, with the exception of some anthocyanin groups that could be involved in its darker black color. In contrast, the Tempranillo negro seeds (Fig. 1C) showed significantly higher concentrations of all the phenolic compounds studied, particularly proanthocyanidins, hydroxycinnamic and hydroxybenzoic acids. Therefore, Tempranillo negro could be considered a somatic variant of Tempranillo altered in the regulation of the phenylpropanoid and stilbene biosynthesis in the seeds. The altered expression of genes involved in those pathways has been reported in other cultivars affected during seed development, as in the case of stenospermocarpic seedless variants, although a chromatographic analysis of the stilbene composition was not carried out (Royo et al., 2018). Thus, the increased phenolic content of Tempranillo negro seeds could be related to the alterations shown in seed development.

Given the differences observed in the phenolic contents in the skin and mainly the seeds of Tempranillo negro, focus was placed on evaluating the phenol extraction during winemaking and ultimately in the phenol composition of derived red wines.

3.2. *Anthocyanins and non-colored phenol extraction from Tempranillo negro berries to musts and fermenting wines during winemaking*

3.2.1. *Anthocyanins*

A wide range of anthocyanins were detected in the musts and fermenting wines (Table 2) with a similar qualitative composition to that detected in the berry skins (Table 1). The concentrations of the anthocyanins determined in the musts were very low (below 1 mg/L) and no statistically significant differences were observed between either Tempranillo clones (Table 2). During winemaking, the maceration of berry skins and seeds contributed significantly to the differentiation of the Tempranillo negro wines, with a higher significant concentration in all anthocyanin subgroups (Table 2). The higher anthocyanin content in Tempranillo negro wines (a 35% increase) does not seem to be related to the total anthocyanin content of the berry skins, which is similar to that observed in the RJ43 clone (Table 1). Such hypotheses as an increase in the skin-to-pulp ratio together with the contribution of seed anthocyanins in the Tempranillo negro could explain this higher anthocyanin content in the wines (Table 2). Nevertheless, after estimating the total anthocyanin content per kg of berries (1004.43 and 993.21 mg/Kg berry fresh weight of RJ43 and VN21 respectively), based on the berry characteristics (Supplementary Tables 1S and 7S), their content was similar in both clones analyzed, which excluded this hypothesis. Given those results, only a higher anthocyanin extractability in the Tempranillo negro can explain the larger contribution of these clones to the

Table 2
Concentration of anthocyanins obtained after targeted profiling by ultra-high performance liquid chromatography with tandem mass spectrometry detection at different phases of the winemaking process, from must to wine, from Tempranillo clone VN21 and from reference RJ43.

Compound[1] (mg/L)	Must			Alcoholic fermentation																		Pressing			Malolactic			Bottling		
	17/09/2019			18/09/2019			19/09/2019			23/09/2019			24/09/2019			25/09/2019			26/09/2019			27/09/2019			25/10/2019			12/11/2019		
	RJ43	VN21	sig	RJ43	VN21	sig	RJ43	VN21	sig	RJ43	VN21	sig	RJ43	VN21	sig	RJ43	VN21	sig	RJ43	VN21	sig	RJ43	VN21	sig	RJ43	VN21	sig	RJ43	VN21	sig
Malvidin-3-glu	0.617	0.331	ns	104.9	128.4	ns	213.3	245.8	*	233.5	269.4	ns	266.5	296.2	ns	201.1	245.9	*	211.3	242.9	*	200.9	211.9	ns	178.1	182.8	ns	182.5	201.1	ns
M−3,5-diglu	n.d.	n.d.	ns	0.452	0.459	ns	3.768	5.282	*	5.114	5.287	ns	5.575	5.950	ns	4.460	5.669	*	5.390	5.945	ns	3.823	5.583	ns	3.712	4.213	ns	1.779	4.209	ns
M−3-(6″-acetyl)-glu	0.348	0.075	ns	16.65	18.38	ns	37.30	42.31	ns	42.58	47.64	ns	50.00	55.72	*	34.56	41.80	ns	37.46	42.03	*	36.47	36.14	ns	32.75	33.14	ns	33.96	38.29	ns
M−3-(6″-coum)-glu	n.d.	n.d.	ns	18.34	13.89	ns	35.41	31.95	ns	28.90	29.18	ns	32.25	32.40	ns	22.38	28.88	*	25.63	29.67	ns	16.34	28.67	ns	20.55	23.11	ns	13.35	24.57	ns
M−3-(6″-caffe)-glu	n.d.	n.d.	ns	0.842	0.664	ns	1.971	1.525	ns	2.794	2.712	ns	4.068	4.721	ns	3.204	4.810	*	4.730	5.605	ns	3.184	5.988	ns	5.179	5.383	ns	2.472	5.957	ns
M−3−arabinoside	n.d.	n.d.	ns	1.760	1.539	ns	2.866	2.764	ns	2.522	2.380	ns	2.714	2.494	ns	1.921	2.172	ns	2.331	2.249	ns	1.411	2.023	ns	1.398	1.423	ns	0.706	1.469	ns
M−3,6-glu-vinylph	n.d.	n.d.	ns	n.d.	0.022	ns	0.041	0.058	ns	0.036	0.038	ns	0.040	0.064	ns	0.013	0.043	*	0.035	0.051	ns	0.005	0.049	*	0.004	0.003	ns	n.d.	0.008	ns
Total Malvidin	**0.965**	**0.406**	**ns**	**143.0**	**163.4**	**ns**	**294.6**	**329.7**	**ns**	**315.5**	**356.6**	**ns**	**361.1**	**397.5**	**ns**	**267.7**	**329.3**	*	**286.8**	**328.4**	*	**262.2**	**290.4**	**ns**	**241.7**	**250.1**	**ns**	**234.7**	**275.6**	*
Petunidin-3-glu	0.005	0.001	ns	15.25	17.76	ns	46.66	66.12	*	51.59	74.00	*	60.51	79.83	**	42.64	61.91	**	44.24	60.13	**	39.04	50.99	ns	41.32	44.168	ns	42.43	49.68	*
Pet-3,5-diglu	n.d.	n.d.	ns	0.023	0.048	ns	0.856	1.728	*	1.291	1.764	*	1.426	1.952	ns	1.070	1.724	**	1.278	1.809	**	0.840	1.646	ns	0.843	1.148	ns	0.310	0.932	*
Pet-3-(6″-acetyl)-glu	n.d.	n.d.	ns	7.518	8.207	ns	18.63	22.60	ns	19.27	21.43	ns	21.06	23.38	ns	15.23	20.76	**	18.37	21.80	*	11.67	20.15	ns	12.72	14.93	ns	6.440	15.57	*
Pet-3-(6″-coum)-glu	n.d.	n.d.	ns	4.216	4.184	ns	13.33	13.96	ns	13.05	13.61	ns	15.39	15.04	ns	9.904	13.14	**	12.08	13.16	ns	7.014	12.25	ns	10.99	10.10	ns	5.931	11.19	ns
Pet-3- arabinoside	n.d.	n.d.	ns	0.090	0.105	ns	0.210	0.246	ns	0.164	0.179	ns	0.174	0.177	ns	0.110	0.144	*	0.110	0.138	*	0.049	0.117	ns	0.060	0.066	ns	0.019	0.077	ns
Total Petunidin	**0.005**	**0.001**	**ns**	**27.10**	**30.30**	**ns**	**79.69**	**104.67**	*	**85.37**	**110.98**	*	**98.56**	**120.39**	*	**68.94**	**97.69**	**	**76.10**	**97.04**	**	**58.61**	**85.15**	**ns**	**65.94**	**70.41**	**ns**	**55.13**	**77.45**	*
Delphidin-3-glu	0.002	0.001	ns	9.112	8.678	ns	33.05	46.63	*	29.91	43.87	**	34.53	43.34	**	22.08	32.19	**	21.58	28.60	**	19.17	23.27	ns	19.24	19.71	ns	20.57	23.08	ns
Del-3,5-diglu	n.d.	n.d.	ns	6.096	6.877	ns	2.954	2.981	ns	1.682	2.025	ns	1.618	2.133	ns	1.333	2.079	*	1.403	2.049	*	1.078	1.923	*	1.109	1.890	*	0.610	1.791	*
Del-3-(6″-acetyl)-glu	n.d.	n.d.	ns	2.343	2.937	ns	8.948	11.88	ns	8.681	10.69	ns	9.632	11.32	ns	6.595	9.790	**	7.624	9.931	**	4.606	9.067	ns	4.995	6.273	ns	2.682	6.867	*
Del-3-(6″-coum)-glu	n.d.	n.d.	ns	1.985	2.002	ns	9.585	10.10	ns	9.124	9.230	ns	11.03	9.809	ns	6.932	8.547	*	7.841	7.890	ns	4.592	7.474	ns	7.367	6.094	ns	4.480	6.814	ns
Total Delphinidin	**0.002**	**0.001**	**ns**	**19.54**	**20.49**	**ns**	**54.54**	**71.59**	*	**49.39**	**65.81**	*	**56.81**	**66.60**	*	**36.94**	**52.61**	**	**38.45**	**48.47**	**	**29.45**	**41.73**	**ns**	**32.71**	**33.97**	**ns**	**28.33**	**38.56**	*
Peonidin-3-glu	0.22	0.144	ns	45.68	56.41	ns	34.67	44.37	*	24.91	36.03	**	25.43	38.11	**	20.43	35.39	**	22.61	36.48	**	16.21	33.87	*	16.25	28.75	**	10.19	29.51	*
Peo-3,5-diglu	n.d.	n.d.	ns	0.083	0.187	ns	0.359	0.823	**	0.330	0.626	**	0.351	0.691	**	0.265	0.635	**	0.318	0.659	**	0.210	0.593	**	0.209	0.475	**	0.086	0.458	*
Peo-3-(6″-acetyl)-glu	n.d.	n.d.	ns	6.725	9.144	ns	9.979	15.99	**	9.247	14.09	**	9.832	15.55	**	7.451	14.25	***	8.783	14.99	***	6.123	13.40	*	6.239	11.317	*	3.421	11.53	*
Peo-3-(6″-coum)-glu	n.d.	n.d.	ns	4.437	6.228	ns	7.274	13.18	***	6.891	11.84	**	7.650	12.86	**	5.302	11.41	***	6.114	11.30	***	3.836	10.33	*	5.441	9.056	*	3.126	9.525	*
Peo-3-arabinoside	n.d.	n.d.	ns	0.211	0.369	ns	0.147	0.198	ns	0.068	0.146	**	0.071	0.144	**	0.031	0.109	**	0.042	0.109	**	0.009	0.090	*	0.007	0.064	**	n.d.	0.068	*
Total Peonidin	**0.220**	**0.144**	**ns**	**57.13**	**72.33**	**ns**	**52.43**	**74.56**	**	**41.45**	**62.74**	**	**43.33**	**67.35**	**	**33.48**	**61.80**	***	**37.87**	**63.54**	***	**26.39**	**58.28**	*	**28.14**	**49.67**	**	**16.82**	**51.09**	*
Cyanidin-3-glu	0.021	0.006	ns	11.83	20.38	ns	2.547	4.276	*	1.513	3.583	**	1.495	3.646	**	1.059	2.943	**	1.129	3.053	**	0.728	2.710	*	0.755	2.281	**	0.369	2.344	*
Cy-3,5-diglu	n.d.	n.d.	ns	0.012	0.017	ns	0.037	0.086	**	0.044	0.078	*	0.045	0.087	*	0.036	0.085	**	0.043	0.086	***	0.030	0.085	**	0.017	0.047	**	0.007	0.041	**
Cy-3-(6″-acetyl)-glu	n.d.	n.d.	ns	1.527	2.762	ns	2.694	5.184	**	2.467	4.449	**	2.583	4.826	**	1.789	4.173	***	2.125	4.367	***	1.330	3.982	*	1.219	2.719	**	0.626	2.881	*
Cy-3-(6″-coum)-glu	n.d.	n.d.	ns	3.136	4.537	ns	6.131	10.50	***	5.619	8.908	**	6.242	9.483	*	3.991	8.171	***	4.549	7.832	***	2.754	7.052	*	4.024	6.035	ns	2.245	6.662	*
Cy-3-arabinoside	n.d.	n.d.	ns	0.022	0.032	ns	0.049	0.087	**	0.042	0.066	**	0.045	0.076	*	0.026	0.065	***	0.029	0.057	***	0.014	0.047	*	0.023	0.038	ns	0.011	0.038	**
Total Cyanidin	**0.021**	**0.006**	**ns**	**16.56**	**27.77**	**ns**	**11.46**	**20.13**	**	**9.686**	**17.09**	**	**10.41**	**18.12**	**	**6.901**	**15.44**	***	**7.875**	**15.40**	***	**4.857**	**13.87**	*	**6.037**	**11.12**	**	**3.257**	**11.97**	*
Pelarg-3,6-diglu	n.d.	n.d.	ns	0.552	1.448	*	0.023	0.048	ns	n.d.	0.027	ns	n.d.	0.026	*	n.d.	0.026	*	n.d.	0.019	*	n.d.	0.020	*	n.d.	0.020	**	n.d.	0.030	*
Vitisin A	n.d.	n.d.	ns	0.111	0.121	ns	0.778	0.748	ns	0.914	0.763	*	1.074	0.914	ns	0.850	0.847	ns	1.078	0.969	ns	0.733	0.955	ns	1.607	1.213	ns	0.853	1.418	ns
Vitisin B	n.d.	n.d.	ns	0.717	2.252	ns	4.299	9.926	***	3.640	4.506	*	3.992	5.129	**	2.792	4.799	***	3.706	5.022	*	2.569	5.294	*	2.116	2.672	ns	0.676	1.979	*
Total Vitisin	**n.d.**	**n.d.**	**ns**	**0.828**	**2.373**	**ns**	**5.077**	**10.67**	***	**4.554**	**5.269**	*	**5.065**	**6.043**	**ns**	**3.642**	**5.647**	***	**4.783**	**5.991**	*	**3.302**	**6.249**	*	**3.723**	**3.885**	**ns**	**1.529**	**3.397**	**ns**
Total Anthocyanins	**1.214**	**0.558**	**ns**	**264.7**	**318.1**	**ns**	**497.8**	**611.3**	*	**505.9**	**618.5**	*	**575.2**	**676.0**	*	**417.6**	**562.5**	***	**451.9**	**558.9**	***	**384.8**	**495.6**	**ns**	**378.2**	**419.1**	**ns**	**339.8**	**458.0**	*

M: malvidin; Pet: petunidin; Del: delphinidin; Peo: peonidin; Cy: cyanidin; Pelarg: pelargonidin; -glu: glucoside; -coum: coumaroyl; caffe: caffeoyl; vinylph: vinylphenol.
Asterisks denote significant differences between clones at the same stage according to Student's *t*-test (P < 0.05, n = 3): *, **and *** indicate significance at $p < 0.05$, $p < 0.01$ and $p < 0.001$, respectively; ns indicates no significant difference, n.d. indicates not detected values.
[1] Standard deviations were lower than 10% (n = 3)

anthocyanin contents of the wine (Table 2). Assuming identical maceration conditions, the extraction rate and extraction coefficient for a given compound will depend largely on the part of the grape. Typically, compounds in the pulp are extracted immediately after crushing, while compounds from the skins will reach a maximum after several days, and compounds from the seeds may take weeks (Waterhouse, Sacks, & Jeffery, 2016). In this sense, variation in the skin structure as well as the abnormal VN21 seed development mentioned above could favor a faster and greater extraction of anthocyanins, which could partly explain the higher anthocyanin contents in the Tempranillo negro wines. In addition, a slightly higher maturity of the VN21 grapes based on °Brix (Supplementary Table 1S) could also contribute to better extractability (Ribéreau-Gayon et al., 2006).

3.2.2. Non-colored phenols

Given the clear differences in the non-colored phenolic compounds in the Tempranillo negro and RJ43 berry skin and seeds (Table 1), it was relevant to evaluate whether those differences could also be observed in the wines. The results showed that concentrations of non-colored phenolic compounds were very low in the musts (Table 3 and Supplementary Table 8S), similarly to that observed for anthocyanins (Table 2). However, starting from the second day of the AF (19/09/2019), the Tempranillo negro wines showed a significantly higher concentration than the RJ43 ones for all non-colored phenolic groups (Table 3), and this was maintained throughout the winemaking process.

Considering the total proanthocyanidins (Table 3 and Supplementary Table 8S), the Tempranillo negro wines highlighted significantly higher concentrations of catechin, epicatechin, dimers and trimers than the RJ43. Their levels in the final bottled wines were two-fold higher in the Tempranillo negro than in the RJ43 wine. These differences could be related to the higher content of proanthocyanidins in the Tempranillo negro seeds (Table 1). Nevertheless, due to the six-fold increase in the total proanthocyanidin concentration in the Tempranillo negro seeds (Table 1), the differences in wines should predictably have been much higher. However, while tannin extraction from the skin is very rapid, reaching a maximum within days, extraction of seed tannins can extend over weeks (Andrich, Zinnai, Venturi, & Fiorentini, 2005) limiting their accumulation in the wines. A similar trend was observed with the flavonols, mainly in the quercetin derivatives, which showed significantly higher concentrations in the VN21 fermenting and the final wines (Table 3).

The major hydroxycinnamic acids found in the fermenting wines were the esters of tartaric acid, such as caftaric acid (caffeoyltartaric acid), coutaric acid (coumaroyltartaric acid) and fertaric acid (feruloyltartaric acid), in parallel with their contents in the skin (Table 3). The concentration of these compounds was higher in the RJ43 than in the Tempranillo negro skin (Table 1), while the opposite was observed in the seeds, musts and wines. Caftaric and fertaric acids were mainly localized in the grape pulp (Garrido & Borges, 2013), and were quickly released into the grape juice (must), as shown in Table 3. On the contrary, coutaric acid, with high concentration in the RJ43 grape skin (Table 1), together with the minor parent hydroxycinnamic acids, caffeic and coumaric, displayed a low concentration in the musts, increasing in the fermenting wines (Table 3) probably via hydroxycinnamate ester hydrolase enzymes (Rentzsch, Schwarz, Winterhalter, & Hermosín-Gutiérrez, 2007) with significant differences being seen between VN21 and RJ43 wines. Variations in the level of hydroxycinnamic acids in the wine cannot be related to their total content in the berry skins, higher in the RJ43 clone than in the VN21 (Table 1). Neither can be explained by the higher VN21 seed content, because the contribution per kg of berries is very similar in both clones (data not shown).

There was up to a ten-fold increase in the concentration of hydroxybenzoic acids during the winemaking process (Table 3). Among these, there was sharp increase in protocatechuic acid, especially after the second day of AF (19/09/2019), and the Tempranillo negro wines showed significantly higher values than the RJ43 ones. The high content of protocatechuic acid in the grape skin and mainly in the seeds (Table 1) could explain its progressive increase during winemaking and the differences observed between the clone wines. Ethyl esters of gallic acid were also identified in wines after AF and mainly after MLF, again at higher concentrations in the Tempranillo negro wines (Table 3). The total hydroxybenzoic acid content in the wine was 1.8 times higher in the VN21 than in the RJ43. This increase could be related to differences in the seed content given the estimation that the level in the VN21 seeds was 1.5 times higher than in the RJ43 ones (Table 1).

Stilbenes were the minor non-colored phenols quantified during the winemaking process from musts to wines (Table 3 and Supplementary Table 8S). The Tempranillo negro must and fermenting wines showed significantly higher concentrations of stilbenes than the RJ43. This difference could be related to the higher stilbene content in the VN21 seeds than the RJ43 seeds, four-fold per kg of seeds or two-fold per kg of berries. The low concentrations of stilbenes detected in the wines studied are within the range of those reported in a recent study by Lukić et al. (2019) among 173 Croatian red and white wines. The differences reported in the trans-piceid concentration between monovarietal red wines (0.78–2.18 mg/L) in that study were similar to those observed between the VN21 (2.278 mg/L) and the RJ43 (0.917 mg/L) wines.

3.2.3. Extraction kinetics of anthocyanins and non-colored phenols in Tempranillo negro fermenting wines comparing with the RJ43 during alcoholic fermentation

Overall, and to better understand the differences in phenolic compounds accumulation observed between Tempranillo negro (VN21) and RJ43 fermenting wines, the extraction of anthocyanins and most representative non-colored phenols (total proanthocyanidins, flavonols and stilbenes) during the AF phase (Fig. 2) was represented. To evaluate the impact of the presence of alcohol on the extractability of these compounds, the density and probable alcohol content (%) of the musts and fermenting wines was determined (Fig. 2A). The density of the VN21 must was significantly higher than that of the RJ43 one, with values of 1110 g/L (26° Brix) and 1100 g/L (24° Brix), respectively (Fig. 1B and 2A). A significant decrease in the density value was observed from the second day of AF (19/09/2019), mainly in the VN21, indicating faster sugar metabolism in the VN21 musts. In parallel, the probable alcohol content increased rapidly, reaching a value of 15.5% (23/09/2019), which then remained almost constant until the end of the AF (27/09/2019) (Fig. 2A). Paradoxically, the AF of the VN21 musts was faster, despite them having a higher sugar content, leaving no residual sugar in the fermenting wine at the end of AF compared with the RJ43 (Fig. 2A).

The trend in the extraction kinetics for anthocyanins and flavonols during AF was similar in both Tempranillo clones (Fig. 2B and D). The total anthocyanin content in both clone musts (Fig. 2B) increased rapidly with the beginning of the AF, reaching its maximum between the 2nd (19/09/2019) and 6th day (24/09/2019). It then remained almost constant until pressing (27/09/2019), which resulted in a slight loss of anthocyanins in the wine. A higher total anthocyanin content on days 2 and 6 in the VN21 wines resulted from significantly higher concentrations of petunidin, delphinidin, peonidin, and cyanidin derivatives (Table 2). At the end of the AF phase (25/09/2019 and 26/09/2019), the VN21 wines displayed greater concentrations of those anthocyanins and higher contents of malvidin derivates when compared with the RJ43 (Table 2). Nevertheless, after MLF (25/10/2019) and immediately before bottling, it was the concentration of peonidin and cyanidinin derivatives that remained significantly higher in the VN21 wines (Table 2), in agreement with the anthocyanin contents observed in the berry skin (Table 1). The observed decrease in anthocyanin content after AF could be the result of their partial re-adsorption on to the skin and other tissue debris (Waterhouse et al., 2016).

Interestingly, the 3% alcohol content reached on day 2 (19/09/2019) in the fermenting wines from both Tempranillo clones (Fig. 2A) appears to be sufficient to promote maximum anthocyanin extraction

Table 3
Concentration of anthocyanins and non-colored phenols (proanthocyanidins, flavonols, hydroxycinnamic acids, hydroxybenzoic acids and stilbenes) obtained after targeted profiling by ultra-high performance liquid chromatography with tandem mass spectrometry detection at different phases of the winemaking process, from must to wine, from Tempranillo clones RJ43 and VN21.

Compound[1] (mg/L)	Must			Alcoholic fermentation																			Pressing			Malolactic			Bottling		
	17/09/2019			18/09/2019			19/09/2019			23/09/2019			24/09/2019			25/09/2019			26/09/2019			27/09/2019			25/10/2019			12/11/2019		
	RJ43	VN21	sig	RJ43	VN21	sig	RJ43	VN21	sig	RJ43	VN21	sig	RJ43	VN21	sig	RJ43	VN21	sig	RJ43	VN21	sig	RJ43	VN21	sig	RJ43	VN21	sig	RJ43	VN21	sig
catechin	0.116	0.025	*	4.571	5.202	ns	8.789	14.56	***	11.93	18.98	***	11.83	20.15	***	10.86	20.25	***	11.15	20.92	***	10.08	20.13	***	9.684	20.03	***	9.696	19.42	***
epicatechin	0.010	0.002	ns	1.183	1.580	ns	2.256	4.041	**	2.642	4.793	***	2.625	5.118	***	2.561	5.404	***	2.618	5.651	***	2.477	5.687	***	2.034	5.485	***	2.003	5.401	***
epicatechin-gal	n.d.	n.d.	ns	0.022	0.015	ns	0.072	0.192	ns	0.161	0.571	*	0.169	0.754	*	0.178	0.854	**	0.225	0.852	**	0.244	0.844	**	0.257	0.205	ns	0.238	0.140	ns
gallocatechin	n.d.	n.d.	ns	0.480	0.084	ns	2.893	3.038	ns	3.807	3.110	**	3.607	2.830	**	3.209	2.699	ns	3.202	2.506	*	2.853	2.235	*	2.698	2.115	*	2.642	2.059	*
epigallocatechin	0.002	0.004	ns	0.127	0.015	ns	1.398	1.987	ns	1.839	1.823	ns	1.725	1.665	ns	1.510	1.472	ns	1.410	1.356	ns	1.267	1.138	ns	1.019	1.074	ns	0.953	1.042	ns
epigallocat-gal	n.d.	n.d.	ns	n.d.	n.d.	ns	n.d.	n.d.	ns	n.d.	0.001	ns	n.d.	0.001	ns	0.001	n.d.	ns	n.d.	0.001	ns	n.d.	n.d.	ns	n.d.	0.001	ns	0.001	0.001	ns
dimers (B1,B2,B3)	0.296	0.150	*	5.404	7.499	*	9.934	16.66	**	13.16	21.18	**	13.72	22.35	**	12.56	22.66	**	13.87	22.72	**	12.86	22.19	**	12.68	22.88	**	12.53	23.08	**
trimer	0.045	0.046	ns	0.060	0.088	ns	0.089	0.138	ns	0.092	0.153	*	0.099	0.152	**	0.099	0.159	*	0.110	0.174	**	0.098	0.177	***	0.096	0.174	**	0.098	0.162	***
Total PA	**0.469**	**0.227**	*	**11.85**	**14.48**	**ns**	**25.43**	**40.62**	***	**33.62**	**50.61**	***	**33.77**	**53.01**	***	**30.98**	**53.51**	***	**32.59**	**54.18**	***	**29.88**	**52.39**	***	**28.47**	**51.96**	***	**28.17**	**51.30**	***
Total quercetins	6.456	5.032	ns	43.57	61.78	*	110.2	147.1	**	119.5	159.5	**	145.6	188.1	**	115.2	165.5	**	131.0	166.6	**	107.4	156.8	**	122.9	128.6	ns	127.4	145.0	*
Total kaempferols	1.390	0.813	ns	16.96	13.25	*	46.80	39.77	*	51.42	39.21	**	58.07	41.74	**	47.44	39.42	*	51.86	35.36	**	45.65	33.92	**	34.64	19.77	**	32.97	19.13	**
Total isorhamnetins	0.416	0.676	ns	4.252	9.555	*	14.06	25.44	**	16.98	29.79	**	20.03	31.52	**	15.49	27.96	**	17.10	27.43	**	13.31	25.69	**	13.74	19.45	*	14.09	19.89	*
Total myricetins	0.043	0.008	ns	4.676	4.820	ns	35.27	45.85	*	38.87	45.13	*	52.51	52.32	ns	32.92	42.54	*	37.72	42.22	ns	25.58	37.30	*	38.53	35.13	ns	36.43	39.54	ns
Others	0.325	0.549	ns	5.072	9.012	*	13.88	20.07	*	14.87	21.26	*	17.79	24.06	*	14.87	22.39	*	16.82	22.98	*	14.56	22.07	*	17.46	20.15	ns	18.13	20.79	ns
Total flavonols	**8.631**	**7.072**	**ns**	**74.53**	**98.42**	**ns**	**220.2**	**278.3**	**	**241.6**	**294.9**	**	**294.0**	**337.8**	**ns**	**225.9**	**297.8**	*	**254.5**	**294.6**	**ns**	**206.5**	**275.7**	*	**227.2**	**223.1**	**ns**	**229.1**	**244.3**	**ns**
caffeic acid	n.d.	0.015	ns	0.060	0.125	ns	0.382	0.849	**	0.364	0.624	*	0.398	0.665	*	0.302	0.642	**	0.366	0.692	**	0.306	0.667	**	0.483	0.842	*	0.475	0.908	*
ethyl-CA	n.d.	n..d	ns	n.d.	n.d.	ns	0.021	0.188	**	0.111	0.536	***	0.172	0.738	***	0.163	0.790	***	0.234	0.895	***	0.204	0.926	***	0.504	1.578	**	0.538	1.665	**
CA-hexose	1.26	1.41	ns	2.495	3.258	*	2.190	2.130	ns	2.130	2.260	ns	2.550	2.780	ns	2.430	2.940	*	2.800	3.190	**	2.910	3.470	*	3.240	3.790	*	3.150	3.750	*
coumaric acid	0.001	0.001	ns	0.022	0.041	ns	0.097	0.260	ns	0.238	0.516	***	0.246	0.510	***	0.241	0.475	**	0.241	0.423	**	0.220	0.357	**	0.336	0.546	*	0.365	0.597	*
CU-hexose	0.633	0.691	ns	1.320	1.450	ns	2.080	2.010	ns	1.960	1.850	ns	2.010	1.940	*	1.900	1.930	ns	2.000	1.900	*	1.980	1.890	ns	1.950	1.820	*	1.960	1.790	*
coutaric acid	0.695	1.836	ns	2.876	4.213	ns	8.883	14.60	*	11.15	15.17	***	10.74	14.22	**	9.725	13.41	*	9.20	12.09	**	8.331	10.38	*	8.348	10.43	*	8.430	10.43	*
caftaric acid	1.330	7.511	**	5.041	9.133	ns	19.27	28.27	**	13.95	20.74	*	15.48	20.58	**	12.08	18.16	**	12.39	17.02	*	9.603	15.00	**	10.39	14.52	*	8.065	13.93	*
ferulic acid	0.002	0.003	ns	0.098	0.172	*	0.221	0.439	***	0.289	0.515	***	0.319	0.550	***	0.302	0.539	***	0.343	0.544	***	0.327	0.546	***	0.315	0.480	***	0.329	0.496	***
fertaric acid	5.380	6.231	ns	7.491	10.42	**	8.434	12.72	**	7.328	10.87	**	8.535	12.32	***	6.515	11.54	***	7.631	11.57	***	6.207	11.01	***	6.355	9.908	**	4.793	9.586	**
Total HC acids	**9.310**	**17.69**	**	**19.40**	**28.81**	**ns**	**41.58**	**61.47**	**	**37.52**	**53.08**	**	**40.45**	**54.31**	**	**33.65**	**50.42**	**	**35.20**	**48.31**	**	**30.09**	**44.25**	**	**31.92**	**43.92**	*	**28.10**	**43.15**	**
gallic acid	0.021	0.007	ns	1.658	2.337	ns	5.177	9.273	***	8.003	15.62	***	9.656	16.64	***	10.02	16.20	***	10.48	17.97	***	10.60	17.95	**	11.24	24.25	***	10.29	23.87	***
GA-glucoside	3.000	2.76	ns	2.435	3.521	ns	1.339	1.679	ns	0.750	1.400	**	0.781	1.479	**	0.733	1.419	**	0.755	1.557	**	0.701	1.568	**	0.342	0.939	**	0.335	0.853	**
methyl-gallate	0.037	0.017	ns	0.343	0.426	ns	0.648	0.806	*	1.007	1.542	ns	1.310	1.770	**	1.571	1.827	ns	1.579	1.937	*	1.805	2.081	ns	1.643	2.107	*	1.547	2.114	*
ethyl-gallate	n.d.	0.002	ns	0.014	0.032	*	0.160	0.654	***	0.411	1.779	**	0.616	2.627	***	0.639	2.825	***	0.882	3.459	***	0.909	3.776	***	1.876	7.133	***	2.032	7.471	***
syringic acid	0.238	0.261	ns	0.526	0.835	*	0.888	1.154	*	0.960	1.469	**	1.150	1.655	**	1.287	1.908	***	1.394	1.903	**	1.584	2.103	**	1.686	2.426	**	1.661	2.412	**
PCT acid	15.47	17.49	*	32.69	55.10	*	132.3	283.2	***	199.9	457.3	**	215.5	421.1	**	227.6	393.2	*	204.3	355.6	***	204.8	328.1	**	197.3	339.4	***	182.4	333.9	**
p-OHB acid	0.005	0.010	ns	0.031	0.046	ns	0.577	0.559	ns	0.029	0.043	*	0.028	0.053	***	0.028	0.059	**	0.035	0.059	*	0.034	0.068	**	0.066	0.090	ns	0.069	0.090	ns
HPA acid	n.d.	n.d.	ns	0.565	0.301	ns	1.227	0.864	ns	0.822	0.970	ns	0.916	0.497	ns	1.006	0.436	ns	0.186	0.705	ns	0.574	0.878	ns	0.332	0.238	ns	0.199	0.023	ns
vanillic acid	0.643	0.856	*	1.373	1.941	***	2.587	3.781	**	2.665	4.040	**	2.960	4.732	**	2.984	4.636	***	2.944	4.619	***	2.897	4.675	**	3.291	4.850	**	3.103	5.141	**
Total HB acids	**19.42**	**21.40**	*	**39.63**	**64.55**	**ns**	**144.6**	**301.9**	**	**214.5**	**484.2**	**	**232.9**	**450.6**	**	**245.8**	**422.6**	**	**222.6**	**387.8**	***	**223.9**	**361.1**	**	**217.8**	**381.4**	***	**201.7**	**375.8**	***
resveratrol *(trans/cis)*	0.009	0.018	ns	0.021	0.100	*	0.064	0.247	***	0.076	0.380	***	0.082	0.400	***	0.092	0.389	***	0.106	0.374	***	0.099	0.311	**	0.095	0.409	**	0.093	0.319	**
piceid *(trans/cis)*	0.021	0.145	*	0.302	1.61	**	1.332	4.717	***	1.531	4.017	***	1.465	3.72	***	1.314	3.393	***	1.366	3.242	***	1.274	3.048	***	1.014	2.618	***	0.917	2.278	***
piceatannol *(trans/cis)*	0.008	0.014	ns	0.011	0.048	*	0.039	0.115	*	0.031	0.074	*	0.032	0.082	*	0.027	0.072	*	0.033	0.070	*	0.056	0.141	*	0.030	0.050	*	0.034	0.059	*
astringin *(trans/cis)*	0.107	0.117	ns	0.097	0.193	*	0.164	0.402	**	0.155	0.224	*	0.158	0.220	*	0.124	0.218	*	0.161	0.184	*	0.179	0.270	*	0.115	0.167	*	0.097	0.152	*
ε-viniferin	0.002	0.003	ns	0.003	0.006	***	0.004	0.015	***	0.010	0.024	***	0.008	0.031	***	0.008	0.033	***	0.009	0.030	***	0.011	0.032	***	0.010	0.035	***	0.010	0.031	***
ω-viniferin	0.002	0.003	ns	0.002	0.003	ns	0.008	0.030	***	0.013	0.046	***	0.015	0.062	***	0.016	0.058	***	0.020	0.060	***	0.020	0.066	***	0.011	0.058	***	0.013	0.042	***
Total Stilbenes	**0.149**	**0.300**	**	**0.436**	**1.960**	*	**1.610**	**5.527**	**	**1.817**	**4.765**	***	**1.759**	**4.515**	***	**1.581**	**4.163**	***	**1.696**	**3.960**	***	**1.639**	**3.868**	***	**1.274**	**3.336**	***	**1.165**	**2.882**	***

PA: proanthocyanidins; HC acids: hydroxycinnamic acids; CA: caffeic acid; CU: coumaric acid; HB acids: hydroxybenzoic acids; GA: gallic acid; PCT: protocatechuic acid; *p*-OHB acid: *p*-hydroxybenzoic acid; HPA: hydroxyphenyl acetic acid

Asterisks denote significant differences between clones at the same stage according to Student's *t*-test (P < 0.05, n = 3): *, **and *** indicate significance at $p < 0.05$, $p < 0.01$ and $p < 0.001$, respectively; ns indicates no significant difference

n.d. indicates not detected values.

[1] Standard deviations were lower than 10% (n = 3)

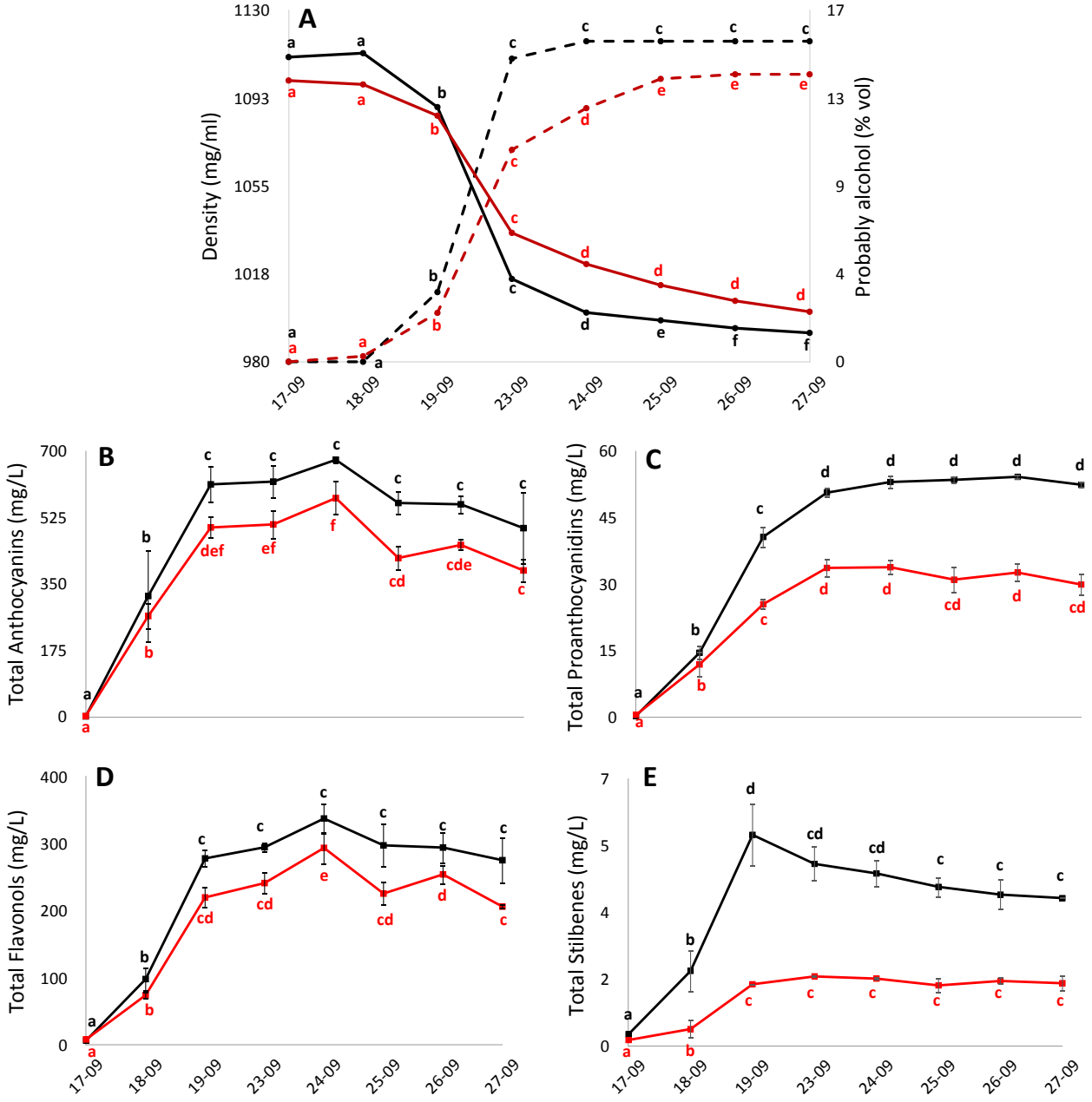

Fig. 2. Phenolic content (mg/L) throughout the alcoholic fermentation of the VN21 and RJ43 musts. A) Evolution of density (g/L) and probable alcohol (%); B) Total anthocyanins; C) Total proanthocyanidins; D) Total flavonols; E) Total stilbenes. The letters indicate statistical differences ($P < 0.05$) between fermenting wines within the same clone (red line: RJ43; black line: VN21). (For interpretation of the references to color in this figure legend, the reader is referred to the web version of this article.)

(Fig. 2B). According to Sacchi, Bisson, and Adams (2005), the limiting factor for releasing anthocyanins is likely to be a physical barrier since they are located in the vacuoles of the hypodermal cells, and extracting them requires that the compounds exit both the membrane-bound vacuole and the cell itself. During fermentation on grape skins, the alcohol content, carbon dioxide and sulfur dioxide, together with the fermentation heat, increase the permeability of the cells and membranes.

The maximum extraction of the more representative non-colored phenols, such as proanthocyanidins, was observed after 6 days AF (24/09/2019) (Fig. 2C), when they reached a plateau. A similar extraction kinetics was seen for phenolic acids (hydroxycinnamic and hydroxybenzoic acids) (data not shown). This differential kinetics reflects the lower solubility of proanthocyanidins in aqueous media compared with anthocyanins, and the need for alcohol in the medium (around 14%) for their effective extraction from the grapes (Fig. 2A). These results are in agreement with previous studies showing that anthocyanin extraction reaches a peak early in fermentation with their concentration dropping thereafter, whereas tannin extraction continues to increase with skin and seed maceration (Sacchi et al., 2005). At the end of AF, the total concentration of the proanthocyanidins decreased slightly after pressing (27/09/2019). This was similar to the drop observed for anthocyanins (Fig. 2B).

Different trends were observed for stilbene extraction kinetics (Fig. 2E) between the Tempranillo negro and the RJ43, the extractability of this phenolic fraction from the grape (skin and seeds) to the fermenting wines being notably low.

Since the winemaking process in our study was identical for both Tempranillo clones, the higher final concentration of anthocyanins and

non-colored phenolic compounds in the Tempranillo negro wines (Fig. 2B) could be explained by the higher concentration of those compounds in the Tempranillo negro berry skin and seeds and/or by improved extractability. As shown in Section 3.2, the estimates of the total anthocyanin and proanthocyanidin contents per kg of berries gave similar total contents in both clones analyzed. So, the higher concentration in the Tempranillo negro wines (35% increase) could result from either a greater extraction capacity of the skin of VN21 berries, or by their slightly advanced ripening stage, given their higher °Brix (Fig. 1B) and derived alcohol content (Fig. 1A), which could help by disrupting cell membranes and improving the release of anthocyanins and non-colored phenols. Further experiments are required regarding the histological analyses of the berry skin and seeds of the Tempranillo negro.

4. Conclusions

This work represents the first attempt to perform an integrative approach combining colorimetric and phenol semi-targeted metabolomic data to improve the knowledge of Tempranillo clone diversity. The dark-black color visually observed in the berries from the singular Tempranillo negro clone (VN21) was confirmed by CIELab chromatic parameters and the targeted chromatographic analysis of berry anthocyanins by UHPLC-QqQ-MS/MS. The higher concentrations of blue-reddish peonidin and cyanidin derivatives in the VN21 grape skin could explain the singular black color of the VN21 berries. In addition, most non-colored compounds from the phenolic family showed increased concentrations in the VN21 seeds, which could be a consequence of their abnormal development. These differences are reflected and even enhanced in the wines, which display higher anthocyanin, proanthocyanidin and stilbene contents. This study exemplifies how spontaneous somatic variation can be used through grapevine clonal selection combining semi-targeted phenol chromatographic analyses.

CRediT authorship contribution statement

Carolina Royo: Formal analysis, Data curation, Methodology, Software, Validation, Visualization. **Yolanda Ferradás:** Formal analysis, Data curation, Methodology, Software, Validation, Visualization. **José Miguel Martínez-Zapater:** Conceptualization, Funding acquisition, Project administration, Resources, Supervision. **Maria-Jose Motilva:** Conceptualization, Resources, Supervision, Writing - original draft.

Declaration of Competing Interest

The authors declare that they have no known competing financial interests or personal relationships that could have appeared to influence the work reported in this paper.

Acknowledgements

This study was financially supported by the Spanish Ministry of Economy and Competitiveness (co-funded by the European Social Fund, European Union) through the grant project BIO2017-86375-R; YF was supported by a grant from the Government of La Rioja; M.J. Motilva thanks the Consejo Superior de Investigaciones Científicas-CSIC for partial funding through the "Ayudas incorporación a escalas científicas CSIC, 2018" (Reference 201870I129).

We would like to thank Vitis Navarra grapevine nursery for donating the grapes; Gobierno de La Rioja experimental winery staff at ICVV; ICVV research group GESVIN led by Rosa López for their wine analytical support; Miguel Ángel Fernández-Recio at the ICVV by his UHPLC-QqQ-MS/MS analytical and technical support in the anthocyanin and phenol analysis and Miguel Angulo by his technical laboratory support.

Appendix A. Supplementary data

Supplementary data to this article can be found online at https://doi.org/10.1016/j.foodchem.2021.130049.

References

Andrich, G., Zinnai, A., Venturi, F., & Fiorentini, R. (2005). A tentative mathematical model to describe the evolution of phenolic compounds during the maceration of Sangiovese and Merlot grapes. *Italian Journal of Food Science, 17*(1), 45–58.

Arrizabalaga, M., Morales, F., Oyarzun, M., Delrot, S., Gomès, E., Irigoyen, J. J., … Pascual, I. (2018). Tempranillo clones differ in the response of berry sugar and anthocyanin accumulation to elevated temperature. *Plant Science, 267*, 74–83. https://doi.org/10.1016/j.plantsci.2017.11.009.

Azuma, A. (2018). Genetic and Environmental Impacts on the Biosynthesis of Anthocyanins in Grapes. *The Japanese Society for Horticultural Science (JSHS), 87*(1), 1–17. https://doi.org/10.2503/hortj.OKD-IR02.

Benbouguerra, N., Richard, T., Saucier, C., & Garcia, F. (2020). Voltammetric Behavior, flavanol and anthocyanin contents, and antioxidant capacity of grape skins and seeds during Ripening (Vitis vinifera var Merlot, Tannat, and Syrah). *Antioxidants, 9*(9), 800. https://doi.org/10.3390/antiox9090800.

Biniari, K., Xenaki, M., Daskalakis, I., Rusjan, D., Bouza, D., & Stavrakaki, M. (2020). Polyphenolic compounds and antioxidants of skin and berry grapes of Greek Vitis vinifera cultivars in relation to climate conditions. *Food Chemistry, 307*, Article 125518. https://doi.org/10.1016/j.foodchem.2019.125518.

Carbonell-Bejerano, P., Royo, C., Torres-Pérez, R., Grimplet, J., Fernandez, L., Franco-Zorrilla, J. M., … Martínez-Zapater, J. M. (2017). Catastrophic unbalanced genome rearrangements cause somatic loss of berry color in grapevine. *Plant Physiology, 175*, 786–801. https://doi.org/10.1104/pp.17.00715.

Castagnoli, S. P., & Vasconcelos, M. C. (2006). Field performance of 20 'Pinot noir' clones in the Willamette Valley of Oregon. *HortTechnology, 16*(1), 153–161. https://doi.org/10.21273/HORTTECH.16.1.0153.

Cuadros-Inostroza, Á., Verdugo-Alegría, C., Willmitzer, L., Moreno-Simunovic, Y., & Vallarino, J. G. (2020). Non-targeted metabolite profiles and sensory properties elucidate commonalities and differences of wines made with the same variety but different cultivar clones. *Metabolites, 10*(6), 220. https://doi.org/10.3390/metabo10060220.

Eshghi, S., Salehi, L., & Karami, M. J. (2014). Antioxidant activity, total phenolic compounds and anthocyanin contents in 35 different grapevine (Vitis vinifera L.) cultivars grown in Fars Province. *International Journal of Horticultural Science and Technology., 1*(2), 151–161. https://doi.org/10.22059/IJHST.2014.52787.

Fang, J., Jogaiah, S., Guan, L., Sun, X., & Abdelrahman, M. (2018). Coloring biology in grape skin: A prospective strategy for molecular farming. *Physiologia Plantarum, 164*(4), 429–441. https://doi.org/10.1111/ppl.12822.

Ferrandino, A., & Guidoni, S. (2010). Anthocyanins, flavonols and hydroxycinnamates: An attempt to use them to discriminate Vitis vinifera L. cv 'Barbera' clones. *European Food Research and Technology, 230*(3), 417–427. https://doi.org/10.1007/s00217-009-1180-3.

Flaginella, L., Di Gaspero, G., & Castellarin, S. D. (2012). Expression of flavonoid genes in the red grape berry of 'Alicante Bouschet'varies with the histological distribution of anthocyanins and their chemical composition. *Planta, 236*(4), 1037–1051. https://doi.org/10.1007/s00425-012-1658-2.

Fraige, K., Pereira-Filho, E. R., & Carrilho, E. (2014). Fingerprinting of anthocyanins from grapes produced in Brazil using HPLC–DAD–MS and exploratory analysis by principal component analysis. *Food Chemistry, 145*, 395–403. https://doi.org/10.1016/j.foodchem.2013.08.066.

García-Estévez, I., Alcalde-Eon, C., & Escribano-Bailón, M. T. (2017). Falavanol quantification of grapes via multiple reaction monitoring mass spectrometry. Application to differentiation among clones of *Vitis vinifera* L. cv. Rufete grapes. *Journal of Agricultural and Food Chemistry, 65*(3), 6359–6368. https://doi.org/10.1021/acs.jafc.6b05278.

Garrido, J., & Borges, F. (2013). Wine and grape polyphenols - A chemical perspective. *Food Research International, 54*(2), 1844–1858. https://doi.org/10.1016/j.foodres.2013.08.002.

Harbone, J. B., Mabry, T. J., & Mabry, H. (Eds.). (1975). *The flavonoids.* London: Chapman & Hall.

He, F., Mu, L., Yan, G. L., Liang, N. N., Pan, Q. H., Wang, J., … Duan, C. Q. (2010). Biosynthesis of anthocyanins and their regulation in colored grapes. *Molecules, 15*(12), 9057–9091. https://doi.org/10.3390/molecules15129057.

Kallithraka, S., Tsoutsouras, E., Tzourou, E., & Lanaridis, P. (2006). Principal phenolic compounds in Greek red wines. *Food Chemistry, 99*(4), 784–793. https://doi.org/10.1016/j.foodchem.2005.07.059.

Lorenz, D. H., Eichhorn, K. W., Bleiholder, H., Klose, R., Meier, U., & Weber, E. (1995). Phenological growth stages of the grapevine (*Vitis vinifera* L. ssp. *vinifera*)—Codes and descriptions according to the extended BBCH scale. *Australian Journal of Grape and Wine Research, 1*(2), 100–110.

Lukić, I., Radeka, S., Budić-Leto, I., Bubola, M., & Vrhovsek, U. (2019). Targeted UHPLC-QqQ-MS/MS profiling of phenolic compounds for differentiation of monovarietal wines and corroboration of particular varietal typicity concepts. *Food Chemistry, 300*, Article 125251. https://doi.org/10.1016/j.foodchem.2019.125251.

Martínez, J., Vicente, T., Martínez, T., Chavarri, J. B. & García-Escudero, E. (2006). Una nueva variedad blanca para la D.O.Ca. Rioja: el Tempranillo Blanco [A new white variety for the DOC Rioja: 'Tempranillo Blanco']. In V. T. Martinez J., Martinez T.,

Chavarri J.B., Garcia-Escudero E., editors (Ed.), 29th OIV World Congress of Vine and Wine 4th General Assembly of the OIV). Logroño, Spain.

Martínez, J. A., Melgosa, M., Pérez, M. M., Hita, E., & Negueruela, A. I. (2001). Note. Visual and instrumental color evaluation in red wines. *Food Science and Technology International, 7*(5), 439–444. https://doi.org/10.1106/VFAT-5REN-1WK2-5JGQ.

Martínez-García, J., Vicente Renedo, T. V., & Martínez Martínez, T. (2000). Comportamiento vitivinícola de los clones de tempranillo seleccionados en La Rioja. *Cuaderno de Campo*, 31–35.

Mattivi, F., Guzzon, R., Vrhovsek, U., Stefanini, M., & Velasco, R. (2006). Metabolite profiling of grape: Flavonols and anthocyanins. *Journal of Agricultural and Food Chemistry, 54*(20), 7692–7702. https://doi.org/10.1021/jf061538c.

Mattivi, F., Vrhovsek, U., Masuero, D., & Trainotti, D. (2009). Differences in the amount and structure of extractable skin and seed tannins amongst red grape varieties. *Australian Journal of Grape and Wine Research, 15*(1), 27–35. https://doi.org/10.1111/j.1755-0238.2008.00027.x.

Mendes Lemos, A., Machado, N., Egea-Cortines, M., & Barros, A. I. (2020). Assessment of quality parameters and phytochemical content of thirty 'Tempranillo' grape clones for varietal improvement in two distinct sub-regions of Douro. *Scientia Horticulturae, 262*(27), Article 109096. https://doi.org/10.1016/j.scienta.2019.109096.

Monagas, M., Gómez-Cordovés, C., Bartolomé, B., Laureano, O., & da Silva, J. R. (2003). Monomeric, Oligomeric, and Polymeric Flavan-3-ol Composition of Wines and Grapes from *Vitis vinifera* L Cv. Graciano, Tempranillo, and Cabernet Sauvignon. *Journal of Agricultural and Food Chemistry, 51*(22), 6475–6481. https://doi.org/10.1021/jf030325+.

Motilva, M. J., Macià, A., Romero, M. P., Rubió, L., Mercader, M., & González-Ferrero, C. (2016). Human bioavailability and metabolism of phenolic compounds from red wine enriched with free or nano-encapsulated phenolic extract. *Journal of Functional Foods, 25*, 80–93. https://doi.org/10.1016/j.jff.2016.05.013.

Muñoz, C., Gomez-Talquenca, S., Chialva, C., Ibáñez, J., Martínez-Zapater, J. M., Peña-Neira, Á., & Lijavetzky, D. (2014). Relationships among Gene Expression and Anthocyanin Composition of Malbec Grapevine Clones. *Journal of Agricultural and Food Chemistry, 62*(28), 6716–6725. https://doi.org/10.1021/jf501575m.

Pantelić, M., Dabić Zagorac, D., Natić, M., Gašić, U., Jović, S., Vujović, D., & Djordjević, J. P. (2016). Impact of clonal variability on phenolics and radical scavenging activity of grapes and wines: A study on the recently developed Merlot and Cabernet Franc Clones (Vitis vinifera L.). *PLoS One, 11*(10), Article e0163823. https://doi.org/10.1371/journal.pone.0163823.

Pinasseau, L., Vallverdú-Queralt, A., Verbaere, A., Roques, M., Meudec, E., Le Cunff, L., … Cheynier, V. (2017). Cultivar diversity of grape skin polyphenol composition and changes in response to drought investigated by LC-MS based metabolomics. *Frontiers in plant science, 8*, 1826. https://doi.org/10.3389/fpls.2017.01826.

Pomar, F., Novo, M., & Masa, A. (2005). Varietal differences among the anthocyanin profiles of 50 red table grape cultivars studied by high performance liquid chromatography. *Journal of Chromatography A, 1094*(1–2), 34–41. https://doi.org/10.1016/j.chroma.2005.07.096.

Rentzsch, M., Schwarz, M., Winterhalter, P., & Hermosín-Gutiérrez, I. (2007). Formation of hydroxyphenyl-pyranoanthocyanins in Grenache wines: Precursor levels and evolution during aging. *Journal of Agricultural and Food Chemistry, 55*(12), 4883–4888. https://doi.org/10.1021/jf0702491.

Restani, P., Fradera, U., Ruf, J.-C., Stockley, C., Teissedre, P.-L., Biella, S., … Lorenzo, C. D. (2021). Grapes and their derivatives in modulation of cognitive decline: A critical review of epidemiological and randomized-controlled trials in humans. *Critical Reviews in Food Science and Nutrition, 61*(4). https://doi.org/10.1080/10408398.2020.1740644.

Revilla, E., García-Beneytez, E., & Cabello, F. (2009). Anthocyanin fingerprint of clones of Tempranillo grapes and wines made with them. *Australian Journal of Grape and Wine Research, 15*(1), 70–78. https://doi.org/10.1111/j.1755-0238.2008.00037.x.

Ribéreau-Gayon, P., Glories, Y., Maujean, A. & Dubourdieu, D. (Eds.). (2006). Handbook of enology, volume 2: The chemistry of Wine Stabilization and Treatments (Vol. 2). John Wiley & Sons.

Rodríguez Montealegre, R., Romero Peces, R., Chacón Vozmediano, J. L., Martínez Gascueña, J., & García Romero, E. (2006). Phenolic compounds in skins and seeds of ten grape Vitis vinifera varieties grown in a warm climate. *Journal of Food Composition and Analysis, 19*(6–7), 687–693. https://doi.org/10.1016/j.jfca.2005.05.003.

Royo, C., Torres-Pérez, R., Mauri, N., Diestro, N., Cabezas, J. A., Marchal, C., … Carbonell-Bejerano, P. (2018). The major origin of seedless grapes is associated with a missense mutation in the MADS-box gene VviAGL11. *Plant Physiology, 177*(3), 1234–1253. https://doi.org/10.1104/pp.18.00259.

Sacchi, K. L., Bisson, L. F., & Adams, D. O. (2005). A review of the effect of winemaking techniques on phenolic extraction in red wines. *American Journal of Enology and Viticulture, 56*(3), 197–206.

Samoticha, J., Jara-Palacios, M. J., Hernández-Hierro, J. M., Heredia, F. J., & Wojdylo, A. (2018). Phenolic compounds and antioxidant activity of twelve grape cultivars measured by chemical and electrochemical methods. *European Food Research and Technology, 244*, 1933–1943. https://doi.org/10.1007/s00217-018-3105-5.

Van Leeuwen, C., Roby, J. P., Alonso-Villaverde, V., & Gindro, K. (2013). Impact of clonal variability in Vitis vinifera cabernet franc on grape composition, wine quality, leaf blade stilbene content, and downy mildew resistance. *Journal of Agricultural and Food Chemistry, 61*(1), 19–24. https://doi.org/10.1021/jf304687c.

Waterhouse, A. L., Sacks, G. L., & Jeffery, D. W. (2016). *(2016) Understanding wine chemistry*. Chichester, West Sussex: John Wiley & Sons Inc.